Journal of Ceramic Processing Research. Vol. 10, No. 2, pp. 235~237 (2009)

J O U R N A L O F
Ceramic Processing Research

Time-Dependent Plasticity of Li_2O-SnO_2-B_2O_3-P_2O_5 Ceramic Glasses

Byoung-Wook Choi, Young-Wook Park, Byung-Gil Yoo, Dong-Wook Shin* and Jae-il Jang*
Division of Materials Science and Engineering, Hanyang University, Seoul 133-791, Korea

The time-dependent plastic deformation (i.e., 'creep') in Li_2O-SnO_2-B_2O_3-P_2O_5 ceramic glasses was probed by nanoindentation creep tests at room temperature. We paid attention to the 'stress exponent (n)' as a major indicator of the room-temperature creep behavior of the ceramic glasses. The estimated stress exponents for steady-state creep are mostly in the range 5~15 and did not significantly change with the indentation peak load.

Key words: Nanoindentation, Creep test, Amorphous Li_2O-SnO_2-B_2O_3-P_2O_5.

Introduction

Sn or SnO_2 based composite materials are candidates for the anode of Li rechargeable battery systems. In spite of their high theoretical capacity, the adoption of these materials into a real battery cell has been hindered by their tremendous initial irreversible capacity severely limiting the cell design [1-4]. The origin of the irreversible capacity is known to be the volume expansion of Sn and subsequent electrochemical interfacial degradation between Sn and the conducting matrix material and the consumption of Li ions during the reduction of SnO or SnO_2 into metallic Sn [5-8]. Therefore, it is quite important that Sn metallic particles maintain mechanical contact to the matrix material during the repetitive charging-discharging processes of battery operation.

The material system Li_2O-SnO_2-B_2O_3-P_2O_5 is expected to exhibit better mechanical integrity compared to other mechanically less flexible materials such as carbon or silicon since the amorphous B_2O_3-P_2O_5 phase is mechanically soft and its volume change is more compatible to Sn-O [9]. Even though the mechanical integrity does not guarantee the electrochemical performance, it is important to understand the time-dependent deformation behavior of this material system to clarify the origin of the electrochemical failure.

Nanoindentation is a popular technique for the estimation of mechanical properties in small volume of a material [10-17]. While hardness and Young's modulus are often measured with the technique, there have been many efforts to estimate the time-dependent plastic deformation using the technique [18-24]. With this in mind, here the time-dependent plastic deformation of the Li_2O-SnO_2-B_2O_3-P_2O_5 ceramic glasses was probed by load relaxation nanoindentation experiments at room temperature.

*Corresponding author:
Tel : +82-2-2220-0402; +82-2-2228-0503
Fax: +82-2-2220-0389
E-mail: jijang@hanyang.ac.kr; dwshin@hanyang.ac.kr

Experimental

Two types of Li_2O-SnO_2-B_2O_3-P_2O_5 ceramic glasses ($7Li_2O$-$65SnO_2$-$14B_2O_3$-$14P_2O_5$ and $7Li_2O$-$60SnO_2$-$16.5B_2O_3$-$16.5P_2O_5$) were examined in this study. High purity reagents of each component of Li_2O-SnO_2-B_2O_3-P_2O_5 were weighed in stoichiometric ratios and mixed thoroughly in a rotary ball mill. Mixed powders were loaded into platinum crucibles and melted in an electric furnace at 1200 °C for 6 h. The platinum crucibles were capped with platinum caps to prevent excessive evaporation of B or P related components. Glass melts were quenched in air and kept in a vacuum dry globe box to prevent possible reactions with moisture in the air. Specimens were polished to an optical grade using polishing oil and CeO_2 powder, and subsequently etched lightly by a 5% HF solution to remove the surface which was possibly damaged during mechanical polishing.

The nanoindentation experiments were carried out under a continuous stiffness measurement (CSM) module of a Nanoindenter-XP (Nano Instruments Inc., Oak Ridge, TN, USA) with a standard Berkovich indenter. Indentation load relaxation tests (schematically shown in Fig. 1) were

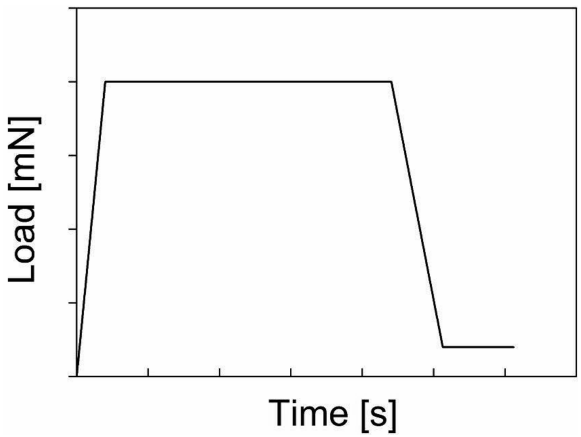

Fig. 1. A schematic illustration of the indentation creep testing procedure.

performed up to different maximum loads in the range from 10 to 200 mN. The holing time at the maximum loads was fixed as 400 s for all experiments while the applied loading rate was varied from 0.1 to 0.5 mN/s.

Results and Disscussion

In this study, we paid attention to the 'stress exponent (n)' as a major indicator for time-dependent deformation (i.e., 'creep') of the ceramic glasses since the steady-state creep in a material is typically described by:

$$\dot{\varepsilon} = A\sigma^n \quad (1)$$

where $\dot{\varepsilon}$ is the strain rate in a uniaxial test, σ is the applied stress, and A is a material constant. Thus, the stress exponent (n) is the reciprocal of the well-known definition of the 'strain rate sensitivity'. From Eq. (1), one can estimate the stress exponent by the relationship, $n = \partial ln(\sigma)/\partial ln(\dot{\varepsilon})$.

Fig. 2 shows representative examples of the indentation creep curves, i.e., (h-h_0) vs. (t-t_0) relation (where h is the indentation displacement, t is the time, and the subscription 0 means the initial status of holding), measured during holding at different peak loads (P_{max}).

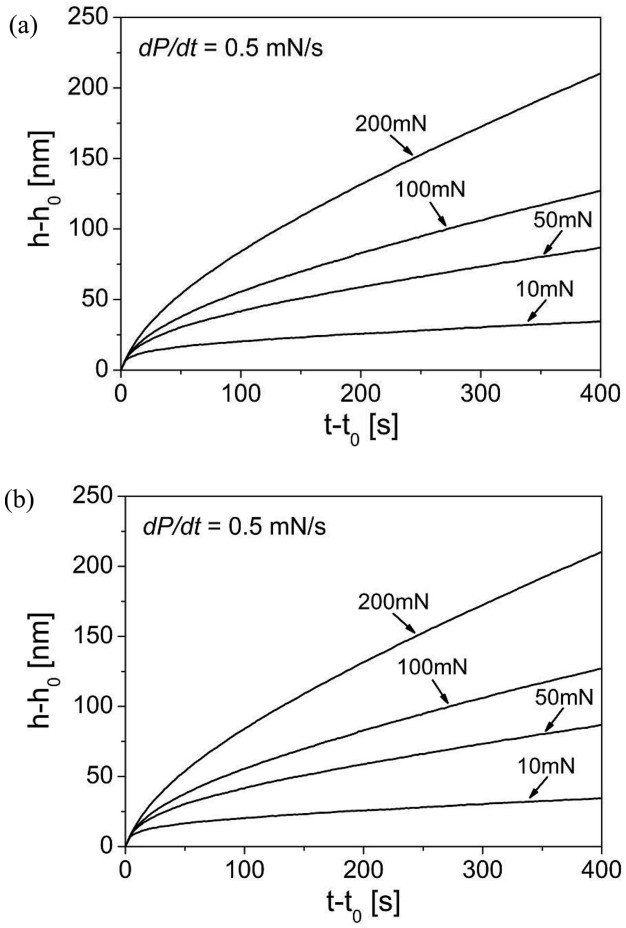

Fig. 2. The experimental data of the creep displacement (h-h_0) vs. hold time (t-t_0) relations for the (a) $7Li_2O$-$65SnO_2$-$14B_2O_3$-$14P_2O_5$, and (b) $7Li_2O$-$60SnO_2$-$16.5B_2O_3$-$16.5P_2O_5$ samples.

As seen in the figure, significant amounts of creep displacements were observed in both samples examined in the present study, and a larger creep displacement (h-h_0) corresponds to a higher P_{max} at a given (t-t_0).

The strain rate in an indentation test ($\dot{\varepsilon}_I$) is usually expressed by [14]:

$$\dot{\varepsilon}_I = \frac{1}{h}\frac{dh}{dt} \quad (2)$$

where h is the indentation depth and t is the time. The displacement rate (dh/dt) in Eq. (2) can be calculated by fitting the h-t curve recorded during holding at the peak load according to the following empirical law [19]:

$$h(t) = h_i + a(t - t_o)^b + kt \quad (3)$$

where h_i (close to h_0, the initial indentation depth), a, b and k are fitting constants, and t_o is the time when the creep process starts. It was revealed that Eq. (3) produces a good fits to most of the results shown in Fig. 2. Also, the was found to decline with time, reaching an approximately steady-state as the dh/dt decreased.

Knowing the contact depth h_c and the contact area A (which are functions of h and h_c respectively), it is possible to evaluate the instantaneous hardness H (which is defined as P/A where P is the indentation load) in a creep process. Then, the representative stress (σ) in Eq. (1) can be estimated from H (which is the same as the mean pressure) by applying Tabor's empirical relation; $H = C\sigma$ where C is a correlation factor which is assumed to be 3 in this study. Note that H, and thus the representative stress σ, are sustained at a given indentation load [10].

To gain the values of the stress exponent $n = \partial ln(\sigma)/\partial ln(\dot{\varepsilon}_I)$, the curves of $\ln(\dot{\varepsilon}_I)$ vs. $\ln(\sigma)$ were drawn, as shown in Fig. 3 (obtained at low and high loads). As shown in the figure, the slopes of the curves parabolically decrease with increasing displacement and decreasing stress. In the steady-state regime (conceivably corresponding to the regime of the end of holding, *i.e.*, the region having a minimum stress value), the slope might indicate the stress exponent for steady-state creep.

Fig. 4 shows the variation in the stress exponent (for different loading rates) as a function of the indentation peak load. For both materials, the estimated stress exponent values are mostly in the range 5~15 (except for one case) and do not seriously change with the indentation peak load. It should be noted that some previous studies reported a strong load-dependency of the exponent values in amorphous materials, which is different from our results. For example, in the case of fused-quartz reported in Refs. [19] and [20], the stress exponent rapidly increased with load and then saturated. This disagreement is possibly due to the difference in the applied peak load; in previous studies, the exponents were mostly obtained at low loads (0.5 mN $\leq P_{max} \leq$ 20 mN), whereas the nanoindentation creep experiments in this study were performed at relatively high loads (10 mN $\leq P_{max} \leq$ 200 mN).

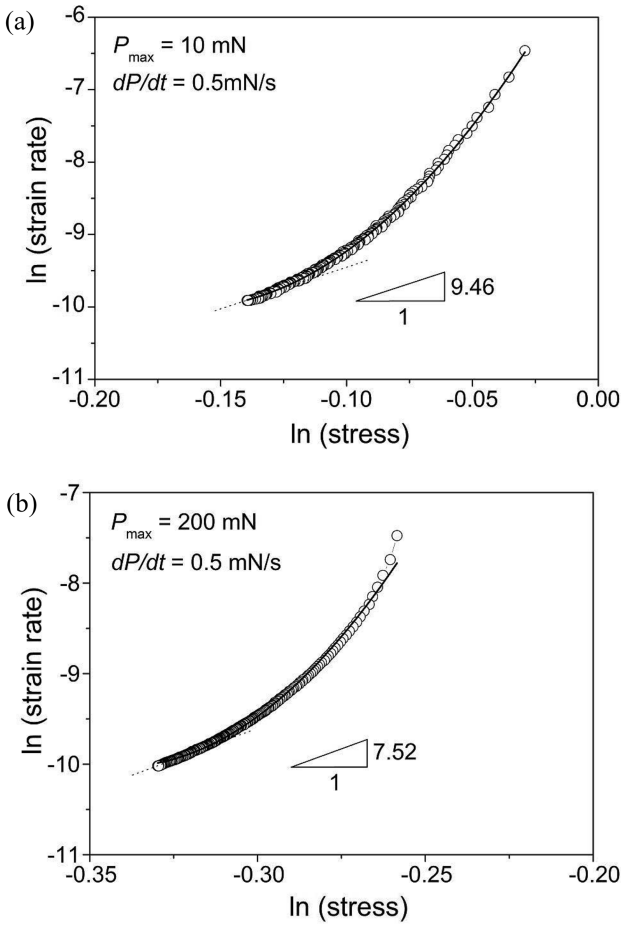

Fig. 3. Representative relation of $\ln(\varepsilon_I)$ vs. $\ln(\sigma)$ of the $7Li_2O$-$65SnO_2$-$16.5B_2O_3$-$16.5P_2O_5$ for different peak loads; P_{max} = (a) 10 mN and (b) 200 mN.

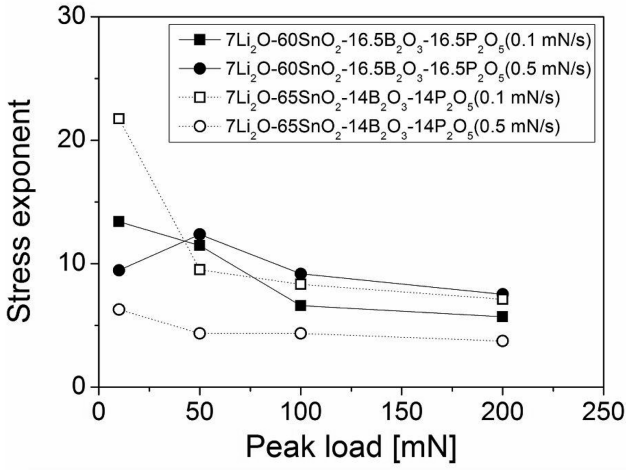

Fig. 4. Variation in steady-state stress exponent as a function of peak load.

Summary

Nanoindentation creep tests were carried out to evaluate the time-dependent plasticity in two types of Li_2O-SnO_2-B_2O_3-P_2O_5 ceramic glasses. The estimated stress exponents for the steady-state creep are mostly in the range 5 ~ 15 and mostly independent of indentation peak load.

Ackowledgement

This research was supported by Hanyang Fusion Materials Program funded by Ministry of Education, Science and Technology, Korea.

Reference

1. Y. Idota, T. Kubota, A. Maekawa and T. Miyasaka, Science 276 (1997) 1395-1397.
2. H. Li, X.J. Huang, L.Q. Chen, Z.G. Wu and Y. Liang, Electrochem. Solid-State Lett. 2 (1999) 547-549.
3. J.Y. Lee, R.F. Zhang and Z.L. Liu, Electrochem. Solid-State Lett. 3 (2000) 167-170.
4. W.H. Lee, H.C. Son, J. Reucroft, J.G. Lee and J.W. Park, J. Mate. Sci. Lett. 20 (2001) 39-41.
5. J. Oh, K. Cho, T. Lee, I. Hwang, S. Jang and D. Shin, J. Ceram. Proc. Res. 9 (2008) 52-56.
6. J. Yang, M. Winter and J.O. Besenhard, Solid-State Ionics 90 (1996) 281-287.
7. J.O. Besenhard, J. Yang and M. Winter, J. Power Sources 68 (1997) 87-90.
8. M. Winter, J.O. Besenhard, M.E. Spahr and P. Novak, Adv. Mater. 10 (1998) 725-763.
9. A.K. Varshneya, in "Fundamentals of Inorganic Glasses" (Academic Press, 1994) p. 87.
10. L.B. Freund and S. Suresh, in "Thin film materials: Stress, Defect Formation and Surface Evolution" (Cambridge University Press, 2004).
11. W.C. Oliver and G.M. Pharr, J. Mater. Res. 7 (1992) 1564-1583.
12. W.C. Oliver and G.M. Pharr, J. Mater. Res. 19 (2004) 3-20.
13. B.N. Lucas and W.C. Oliver, Metall. Mater. Trans. A 30 (1999) 601-610.
14. W.H. Poisl, W.C. Oliver and B.D. Fabes, J. Mater. Res. 10 (1995) 2024-2032.
15. A.A. Elmustafa and D.S. Stone, J. Mech. Phys. Sol. 51 (2003) 357-381.
16. C.A. Schuh and T.G. Nieh, J. Mater. Res. 19 (2004) 46-57.
17. J.L. Hay and G.M. Pharr in "Instrumented Indentation Testing" (ASM Handbook, 2000) p.232.
18. H. Li and A.H.W. Ngan, Scripta Mater. 52 (2005) 827-831.
19. H. Li and A.H.W. Ngan, J. Mater. Res. 19 (2004) 513-522.
20. Z. Cao and X. Zhang, Scripta Mater. 56 (2007) 249-252.
21. G. Feng and A.H.W. Ngan, J. Mater. Res. 17 (2002) 660.